# III

Publication III

S. Sillanpää and M. Heinonen, The contribution of varying shear stress to the uncertainty in gravimetric gas mass flow measurements, Metrologia **45**, 249 - 255 (2008).



http://www.iop.org/journals/met
http://stacks.iop.org/met/45/249

IOP PUBLISHING METROLOGIA
Metrologia **45** (2008) 249–255 doi:10.1088/0026-1394/45/2/015

# The contribution of varying shear stress to the uncertainty in gravimetric gas mass flow measurements

**Sampo Sillanpää and Martti Heinonen**

Centre for Metrology and Accreditation (MIKES), PO Box 9, FI-02151 Espoo, Finland

E-mail: sampo.sillanpaa@mikes.fi and martti.heinonen@mikes.fi

Received 20 August 2007
Published 31 March 2008
Online at stacks.iop.org/Met/45/249

**Abstract**

The effect of natural convection on the uncertainty calculation of the MIKES dynamic gravimetric gas mass flow measurement system (DWS) is studied in this paper. The magnitude of the uncertainty component due to varying shear stress rate at the wall of the cylinder is studied theoretically at two different varying temperature models. Based on the obtained results, the contribution of the component may be significant, if the temperature difference between the wall of a gas cylinder and ambient air increases 1 K during one measurement cycle. Then the contribution of the shear stress can be above 92% of the combined standard uncertainty at the gas mass flow rate 0.1 mg $s^{-1}$. Correspondingly, the contribution at the same temperature difference is below 1% at the mass flow rate 625 mg $s^{-1}$. Applying the Monte Carlo uncertainty estimation method, the assumption of independent variables was shown to be reasonable.

## 1. Introduction

A dynamic gravimetric mass flow determination provides a fundamental method to calibrate small gas flow meters: the gas mass flow rate value is determined solely from mass and time measurements. Thus, this method establishes a traceability link from flow measurements to realizations of mass and time units. The dynamic determination means that a gas vessel placed on a weighing pan of a balance is continuously weighed while gas is flowing out from the vessel. The mean gas mass flow rate can be obtained from recorded mass and time values, for example by calculating the slope of the linear fitting of the air buoyancy corrected balance indications over time values.

In mass measurements, the effect of convective forces is minimized by letting a weight and the balance reach thermal equilibrium if possible. Gläser and Do [1] studied the effect of these forces on the apparent masses of different mass standards as a function of temperature and time. In another paper by Gläser [2], appropriate waiting times for different types of weights are concluded from studies on heat transfer effects around different mass standards. After the appropriate waiting times, the thermal equilibrium is assumed to be achieved and the effect of convective forces can be neglected. Löfström [3] studied the manufacturing of gas compositions by the weighing method. He also studied the response of an apparent mass to thermal gradients [3] and presented an equation for the mass change of a cylindrical surface due to convective forces as

$$\delta m_c = CAh^{\frac{1}{4}}\Delta T^n. \quad (1)$$

In equation (1) $\delta m_c$, $A$, $h$ and $\Delta T$ are the change in the balance indication due to natural convection in grams, the vertical surface area of the cylinder in square centimetres, the height of the cylinder in centimetres and the temperature difference between the wall of the cylinder and ambient air, respectively. Constants $C = -9.2 \times 10^{-7}$ g $cm^{-2.25}$ $K^{-1}$ and $n = 1$.

The apparent mass change due to the natural convection of ambient air has been studied numerically with the CFD-program by Mana *et al* in [4]. They found that the experimental and numerical results were in reasonable agreement. They also derived sensitivity coefficients for a mass change as a function of temperature for a 1 kg stainless steel mass standard and a spherical density standard made of silicon.

In contrast to precision mass measurements, thermal equilibrium cannot be reached in gas mass flow measurements because the flow measurement process is highly dynamical by nature. When gas flows out from the gas vessel, the gas pressure in the vessel decreases. This in turn induces a

  

temperature drop in the vessel. The thermal non-equilibrium between the gas vessel wall and ambient air continuously increases during the measurement. The natural convection flow induced by the temperature difference causes shear stress on the wall of the vessel. It varies as a function of temperature difference between the wall and ambient air.

The smaller is the mass flow rate the stronger the effect of varying shear stress that can be detected, because of the small gas mass loss from the vessel during one measurement cycle. At mass flow rates less than 21 mg s$^{-1}$, a quite long measurement time (>400 s) is needed to obtain the mass loss required to achieve a good accuracy. Usually, however, thermal non-equilibrium at the very small gas mass flows is not generated by a fast pressure drop but more probably by inadequate temperature stabilization after the cylinder filling or rapid fluctuations of the temperature of ambient air.

In a previous study at MIKES, the effect of the natural convection flow was experimentally investigated by inducing a thermal non-equilibrium between the gas vessel wall and ambient air and then allowing the system to reach equilibrium. The order of magnitude for the effect was found by monitoring the temperature difference and indications of the balance as a function of time [5]. This was included in the uncertainty budget after multiplying by a safety factor of two.

To increase our knowledge of the natural convection effect, further theoretical and experimental investigations have been carried out at MIKES [6]. The obtained results provide a good basis for improving the uncertainty analysis of the MIKES primary flow standard (DWS).

In this work, shear stress on a cylindrical wall in a time dependent situation is calculated using the similarity solution of laminar boundary layer equations. This calculation method is presented in [6], where theoretical results were validated through experimental results. In the analysis, it is assumed that the temperature of the wall is known as a function of time during the gas mass flow measurement. The estimate for the total effect of varying shear stress on the measurement result is obtained as a time average of instantaneous shear stress rates on the cylinder wall. The method presented in [6] can be applied to the cylinders mounted vertically (the bottom of the cylinder on the weighing pan of the balance) or horizontally (the longest side on the weighing pan).

If the gas pressure decreases fast, the wall of the cylinder cools down rapidly and the water vapour from laboratory air can condense onto the wall. This phenomenon near the dew-point is not, however, included in this study.

In this paper, the calculation of standard uncertainty for the MIKES dynamic gravimetric gas mass flow standard is first briefly presented. Then the estimation of the uncertainty component due to natural convection flow is described. The significance of this component is studied by calculating the combined uncertainty of the gas flow standard in four cases with two different temperature difference models. The numerical Monte Carlo method (MCS) was applied to study the possible effect of correlation and to validate the obtained uncertainty calculation based on the law of propagation of uncertainty (LPU). As an example of the validation process, the Monte Carlo procedure was applied to the flow rate of 0.1 mg s$^{-1}$.

## 2. Uncertainty analysis method

### 2.1. Mathematical model for generated gas mass flow

In a dynamic gravimetric gas flow standard, the instantaneous net force $F$ acting on the load cell of a balance is

$$F = m_t \left(1 - \frac{\rho_a}{\rho_t}\right) g + \delta F_T + \delta F_C + \delta F_L, \tag{2}$$

where $m_t$, $\rho_a$, $\rho_t$, $g$, $\delta F_T$, $\delta F_C$ and $\delta F_L$ are the true mass of the gas cylinder, the density of the surrounding air, the effective density of the gas cylinder, the acceleration due to gravity, the sum of forces caused by the connecting tube, the force due to natural convection and the force due to leakage out of the gas cylinder, respectively. The indication of the balance $I$ is $I = L + \delta I$, where $L$ is the net force divided by the local acceleration of the gravity and $\delta I$ includes errors due to balance mechanics (resolution, linearity, stability and zeroing). Thus it can be written

$$I = \alpha m_t \left(1 - \frac{\rho_a}{\rho_t}\right) + \delta I + \delta m_T + \delta m_C + \delta m_L, \tag{3}$$

where $\alpha = (1 - \rho_{a0}/\rho_r)^{-1}$, $\rho_{a0} = 1.2\,\mathrm{kg\,m^{-3}}$, $\rho_r = 8000\,\mathrm{kg\,m^{-3}}$ and $\delta m_T$, $\delta m_C$, $\delta m_L$ are contributions to the indication due to the connecting tube, natural convection and leakage, respectively. The true mass of the gas cylinder is

$$m_t = \frac{I - \delta I - \delta m_T - \delta m_C - \delta m_L}{\alpha \left(1 - \frac{\rho_a}{\rho_t}\right)}. \tag{4}$$

By writing the total differential of (4) and dividing it by a differential time d$t$, one gets the mass flow

$$\dot{m}_t = \beta \left[\dot{I} - \delta\dot{I} - \frac{m_t}{\rho_t}\dot{\rho}_a - \frac{m_t \rho_a}{\rho_t^2}\dot{\rho}_t - \delta\dot{m}_T - \delta\dot{m}_C - \delta\dot{m}_L\right], \tag{5}$$

where $\beta = (\alpha(1 - \rho_a/\rho_t))^{-1}$.

When applying equation (5) to a dynamic weighing based system, a large number of consecutive short time intervals are studied and the following discrete approximation is used:

$$\dot{m}_t \approx \frac{\beta}{\Delta t}[\Delta I - \Delta\delta I - m_t \Delta\rho_a/\rho_t - m_t \Delta\rho_t \rho_a/\rho_t^2 - \Delta\delta m_T - \Delta\delta m_C - \Delta\delta m_L]. \tag{6}$$

Sensitivity coefficients are derived from equation (6) for the calculation of the combined standard uncertainty. The uncertainty components are presented in table 1. In practical calculations, the uncertainty component $u(\Delta\rho_t)$ and the uncertainty of acceleration due to gravity are assumed to be so small that they can be neglected. Assuming that all variables are independent of each other, the combined standard uncertainty is calculated in the following way [7]:

$$u_c^2(\dot{m}_t) \approx u_c^2(\Delta m_t) = \sum_{i=1}^{10} c_i^2 u^2(y_i). \tag{7}$$

An example of the uncertainty budgets can be found from table 2.

**Table 1.** Uncertainty components.

| $i$ | $y_i$ | Unit | Annotation |
|---|---|---|---|
| 1 | $u(\Delta\delta I)$ | kg | Resolution of the balance and its stability |
| 2 | $u(\Delta I)$ | kg | Gas mass difference, including contributions due to a balance nonlinearity and a standard deviation of the mean of the difference between the linear fit of the balance indications and the instantaneous indication of the balance |
| 3 | $u(\rho_a)$ | $kg\,m^{-3}$ | Air density |
| 4 | $u(\Delta\rho_a)$ | $kg\,m^{-3}$ | Air density change during the measurement |
| 5 | $u(\rho_t)$ | $kg\,m^{-3}$ | Density of the gas cylinder |
| 6 | $u(\Delta\rho_t)$ | $kg\,m^{-3}$ | Density change of the gas cylinder during the measurement |
| 7 | $u(\Delta t)$ | s | Time measurement |
| 8 | $u(\Delta\delta m_T)$ | kg | Effect of connection tube during the measurement |
| 9 | $u(\Delta\delta m_c)$ | kg | Effect of natural convection during the measurement |
| 10 | $u(\Delta\delta m_L)$ | kg | Leakage out of the system during the measurement |

**Table 2.** Uncertainty budgets at different gas mass flow rates at $\Delta T = 1$ K.

| $c_i u(y_i)$/ ($mg\,s^{-1}$) | $q_m$/($mg\,s^{-1}$) | | | |
|---|---|---|---|---|
| | 625 | 312 | 21 | 0.1 |
| $c_1u(y_1)$ | $1.6 \times 10^{-6}$ | $8.4 \times 10^{-7}$ | $9.0 \times 10^{-9}$ | $6.3 \times 10^{-10}$ |
| $c_2u(y_2)$ | 0.05 | 0.2 | $2.1 \times 10^{-4}$ | $7.9 \times 10^{-6}$ |
| $c_3u(y_3)$ | $1.4 \times 10^{-3}$ | $6.8 \times 10^{-4}$ | $1.0 \times 10^{-5}$ | $4.8 \times 10^{-8}$ |
| $c_4u(y_4)$ | $2.2 \times 10^{-5}$ | $6.3 \times 10^{-6}$ | $6.1 \times 10^{-8}$ | $4.7 \times 10^{-11}$ |
| $c_5u(y_5)$ | 0.006 | $4.3 \times 10^{-3}$ | $4.1 \times 10^{-4}$ | $5.1 \times 10^{-6}$ |
| $c_6u(y_6)$ | 0 | 0 | 0 | 0 |
| $c_7u(y_7)$ | 0.06 | 0.03 | $2.1 \times 10^{-3}$ | $9.8 \times 10^{-6}$ |
| $c_8u(y_8)$ | 0.7 | 0.3 | 0.01 | $1.2 \times 10^{-4}$ |
| $c_9u(y_9)$ | 0.06 | 0.02 | $2.6 \times 10^{-3}$ | $4.6 \times 10^{-3}$ |
| $c_{10}u(y_{10})$ | $2.9 \times 10^{-4}$ | $2.9 \times 10^{-4}$ | $5.8 \times 10^{-5}$ | $5.8 \times 10^{-5}$ |
| $u_c$[a] | 0.72 | 0.33 | 0.014 | 0.0005 |

[a] Combined standard uncertainty.

### *2.2. An improved method for estimating the effect of natural convection flow*

As shown in [6], the time average equation can be used as the estimate of varying convective forces (shear stress rate) during one measurement cycle

$$\delta\dot{m}_c = \frac{d}{dt}\int\left[\frac{1}{g(t-t')}\int_{t'}^{t}\tau_w(\Delta T(t))\,dt\right]dA. \qquad (8)$$

Here, $t - t'$ is the measurement time and $\tau_w(\Delta T(t))$ the gas cylinder wall shear stress as a function of temperature difference. The instantaneous shear stress rate at the wall of the gas cylinder is calculated as follows:

$$\tau_w = \rho_a \nu \frac{du}{dy} = \frac{2\mu}{x}[x\beta g\Delta T(t)]^{\frac{1}{2}}\left(\frac{Gr_x}{4}\right)^{\frac{1}{4}} f''(0), \qquad (9)$$

where $\nu$ is the kinematic viscosity, $u$ the velocity along a surface of the cylinder, $\mu$ the absolute viscosity, $\beta g$ the buoyancy parameter, $\Delta T(t)$ the temperature difference between the cylinder wall and ambient air at the time $t$ and $Gr_x$ local Grashof number at the distance $x$ from the leading edge [6]. The second derivative at zero of the dimensionless similarity function is calculated by solving numerically the set of coupled non-linear differential equations (10) and (11) [8,9]. These equations give a similarity solution for a laminar two-dimensional boundary layer equations.

$$f''' + (3+m+n)ff'' - 2(1+m+n)f'^2 + \Theta = 0, \qquad (10)$$

$$\Theta'' + (3+m+n)Pr\ f\Theta' - 4m\ Pr\ f'\Theta = 0. \qquad (11)$$

In equations (10) and (11), primed quantities indicate differentiation with respect to a similarity parameter $\eta$, and $Pr$ is the Prandtl number. Variables $f$ and $\Theta$ are functions of $\eta$ with boundary and initial conditions

$$f(0) = f'(0) = f'(\infty) = 0, \qquad (12)$$

$$\Theta(0) = 1 \qquad \Theta(\infty) = 0. \qquad (13)$$

The gas cylinder wall temperature is assumed to obey the power law. Therefore, the standard cases are determined by $m = 0$ ($T_w$ is a constant) and $m = 1/5$ (heat flux $q_w$ is a constant). Each value of $n$ corresponds to a particular body contour. For $n = 0$, a flat plate is obtained, which is used for calculating the velocity profile around a gas cylinder placed vertically on a balance. The value $n = 1$ corresponds to the stagnation point flow along a rounded surface, for example a circular gas cylinder placed with the longest side on the weighing pan of a balance.

With equation (8), it is possible to obtain an uncertainty estimate for the effect of natural convection flow after

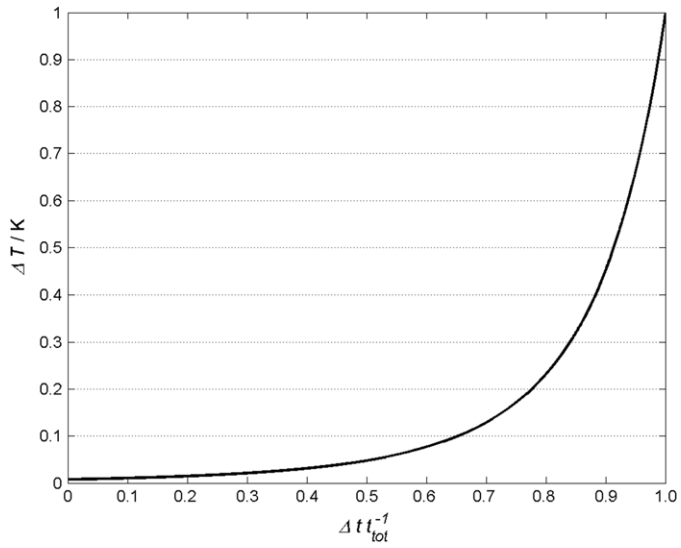


**Figure 1.** The temperature difference model between the wall of the gas cylinder and ambient air as a function of a dimensionless measurement time. The model was used for simulating a situation where the temperature of the gas vessel or ambient air increases or decreases during a measurement cycle.

completing the measurement. It is assumed that an adequate number of grid node points is used to get a grid independent numerical solution of the boundary and initial value problem (equations from (9) to (13)). Then the numerical calculation uncertainty is negligible.

## 3. The contribution of natural convection flow to the combined standard uncertainty

To study the significance of the natural convection in the uncertainty budget at different mass flow rates, the presented theory was implemented as a computer code. Calculations were carried out for two cases with different time dependences of the temperature difference between the gas vessel and ambient air. In the first one the dependence was obtained using a theoretical model which was developed for calculating the thermal stabilization times for weights [2]. Here, the total change in the temperature difference between the wall and ambient air during the time period of interest was 1 K. The temperature difference as a function of measurement time is presented in figure 1. This temperature model was used for simulating a situation where the temperature of the gas vessel or ambient air increases or decreases during a measurement cycle. In the second case, the temperature difference was assumed to change in the same way as measured inside the wind shield of the MIKES system very near the wall of the gas vessel during one gas mass flow measurement. As can be seen from figure 2, the temperature difference fluctuated around the initial temperature value less than $\pm 0.2$ K. This temperature difference model simulates weighing conditions without any major temperature increase or decrease.

In the calculation of measurement results, the effect of varying shear stress rate is taken into account only in the measurement uncertainty, i.e. the estimate of $\delta m_C$ is assumed to be zero but its uncertainty is included in the uncertainty budget. Therefore, the effect of varying shear stress can only be seen in the change in the combined standard uncertainty.

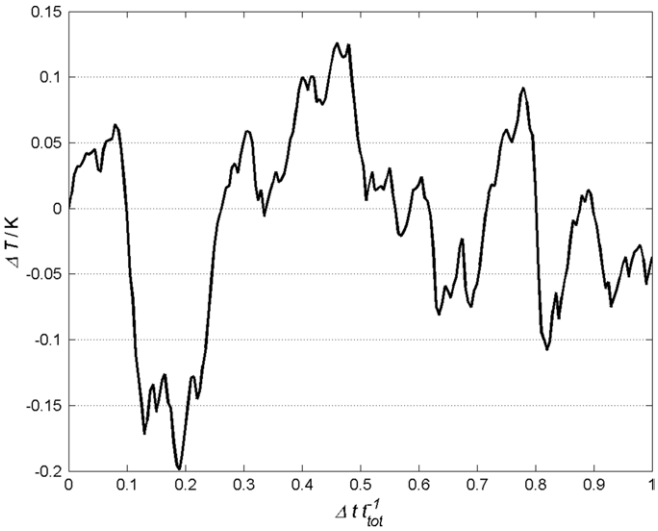


**Figure 2.** The temperature difference model between the wall of the gas cylinder and ambient air as a function of a dimensionless measurement time. The model was used for simulating normal measurement situation.

When comparing the uncertainty calculations obtained with the two temperature difference models, all other uncertainty components except the one related to the shear stress were assumed to be constant in all cases. Only the calculation method for $u(\Delta\delta m_C)$ and the temperature difference model were changed.

In the calculations, four different mass flow rates were studied: 0.1 mg s$^{-1}$, 21 mg s$^{-1}$, 312 mg s$^{-1}$ and 625 mg s$^{-1}$. The corresponding uncertainties for all mass flow rates were calculated using four different values for $u(\Delta\delta m_C)$. In the first case, the temperature difference model was adjusted giving $\Delta T = 1$ K during one measurement cycle. Also the varying shear stress was taken into account as in equation (8). The second case was similar to the first one, but now the second temperature difference model ($\Delta T = 0.2$ K) was used. The

third case was calculated by omitting the shear stress effect and using the same temperature difference model ($\Delta T = 1$ K) as in the first case. The last case was similar to the third one, except now the second model was used giving $\Delta T = 0.2$ K at maximum. An example of the uncertainty budgets in the first case is given in table 2.

The summary of combined standard uncertainties from calculated test cases is presented in table 3. At the mass flow rate of 625 mg s$^{-1}$, the differences between the largest and the smallest calculated mass flow values were within 0.01 mg s$^{-1}$, corresponding to an increase of less than 0.01% in combined standard uncertainty. For the mass flow rate of 312 mg s$^{-1}$ the corresponding differences were 0.01 mg s$^{-1}$ and 0.01%. At the mass flow rate of 21 mg s$^{-1}$ there were no significant differences in mass flow rates, but a 0.01% increase in uncertainties at the maximum. The analysis of the smallest mass flow rate of 0.1 mg s$^{-1}$ showed that the uncertainties were between 0.49% in the first calculation case and 0.13% at the minimum and there was no significant alteration in mass flows.

Tables 4 and 5 present individual relative contributions of each uncertainty component to the combined standard uncertainty. In the tables, numbering of the uncertainty components in the first column refers to the numbering used for each uncertainty component in table 1. Components are compared with each other in the above described four test cases and four different mass flow rates. Percentages in the tables are obtained by dividing each squared product of the uncertainty component and its sensitivity coefficient by the sum of squares of all ten components:

$$c_i^* u_i^* = \frac{c_i^2 u_i^2}{\sum_{i=1}^{10} c_i^2 u_i^2} \times 100\%. \qquad (14)$$

**Table 3.** The summary of combined standard uncertainties for the studied four test cases.

| Case | 625 mg s$^{-1}$ $u_c \times 100$ | 321 mg s$^{-1}$ $u_c \times 100$ | 21 mg s$^{-1}$ $u_c \times 100$ | 0.1 mg s$^{-1}$ $u_c \times 100$ |
|---|---|---|---|---|
| 1 | 0.12 | 0.11 | 0.08 | 0.49 |
| 2 | 0.12 | 0.10 | 0.07 | 0.17 |
| 3 | 0.12 | 0.10 | 0.07 | 0.13 |
| 4 | 0.12 | 0.10 | 0.07 | 0.13 |

The uncertainty component due to the connection tube ($\Delta\delta m_T$) usually has the largest contribution to the combined standard uncertainty, as can be seen from tables 4 and 5. However, if the temperature condition during the measurement cycle is not stable, the situation can be different, as can be seen from table 4. At the gas mass flow rate 0.1 mg s$^{-1}$, even small temperature differences during the measurement cycle can increase the combined standard uncertainty significantly. When the calculation model for the shear stress was not in use, in tables 4 and 5, the contribution of shear stress is zero. At the gas mass flow rates larger than 200 mg s$^{-1}$, the risk of increasing temperature difference between the cylinder wall and ambient air grows dramatically. This is due to fast pressure loss in the gas cylinder causing the gas cooling. However, the gas mass loss from the cylinder is so large that the effect of varying shear stress almost vanishes. This can be seen from table 5, where the uncertainty of the connecting tube is dominating at the temperature difference of 1 K.

## 4. Numerical method for calculating the approximation for a standard uncertainty of DWS

As can be seen, the air temperature measurement at the boundary layer of a gas cylinder is used for calculating both the shear stress on the cylinder wall and the air density for buoyancy correction of the indication of the balance. However, the use of equation (7) assumes independent uncertainty components. To ensure that the assumption of independent variables is tenable, the measurement uncertainty for DWS was calculated numerically as well. The numerical method was based on Monte Carlo simulation and was carried out according to [10].

The simulation was carried out for a gas mass flow rate of 0.1 mg s$^{-1}$ at a temperature difference of 1 K, because at these conditions the effect of varying shear stress was found to be the most pronounced among the studied cases. The simulation method for other flow rates is similar.

In the simulation, 10 000 Monte Carlo trials were calculated. The input variables used and their distributions are listed in table 6. In every trial, the air density was calculated using the equation presented in [11] and the true mass of the gas cylinder was obtained with the help of equation (4). The

**Table 4.** Comparison of the contribution of different uncertainty components with the combined standard uncertainty at mass flow rates of 0.1 mg s$^{-1}$ and 21 mg s$^{-1}$.

| | 0.1 mg s$^{-1}$ | | | | 21 mg s$^{-1}$ | | | |
|---|---|---|---|---|---|---|---|---|
| $\Delta T$ | 1 K | 0.2 K | 1 K | 0.2 K | 1 K | 0.2 K | 1 K | 0.2 K |
| $u(\Delta\delta m_c)$ | Yes | Yes | No | No | Yes | Yes | No | No |
| $c_1u(y_1)$ | 0.00 | 0.00 | 0.00 | 0.00 | 0.00 | 0.00 | 0.00 | 0.00 |
| $c_2u(y_2)$ | 0.03 | 0.23 | 0.36 | 0.36 | 0.03 | 0.03 | 0.03 | 0.03 |
| $c_3u(y_3)$ | 0.00 | 0.00 | 0.00 | 0.00 | 0.00 | 0.00 | 0.00 | 0.00 |
| $c_4u(y_4)$ | 0.00 | 0.00 | 0.00 | 0.00 | 0.00 | 0.00 | 0.00 | 0.00 |
| $c_5u(y_5)$ | 0.01 | 0.10 | 0.15 | 0.15 | 0.09 | 0.09 | 0.09 | 0.09 |
| $c_6u(y_6)$ | 0.00 | 0.00 | 0.00 | 0.00 | 0.00 | 0.00 | 0.00 | 0.00 |
| $c_7u(y_7)$ | 0.04 | 0.36 | 0.56 | 0.56 | 2.32 | 2.35 | 2.41 | 2.41 |
| $c_8u(y_8)$ | 5.98 | 51.12 | 79.52 | 79.52 | 93.94 | 95.09 | 97.47 | 97.47 |
| $c_9u(y_9)$ | 92.48 | 35.72 | 0.00 | 0.00 | 3.62 | 2.44 | 0.00 | 0.00 |
| $c_{10}u(y_{10})$ | 1.46 | 12.48 | 19.41 | 19.41 | 0.00 | 0.00 | 0.00 | 0.00 |

**Table 5.** Comparison of the contribution of different uncertainty components with the combined standard uncertainty at mass flow rates of 312 mg s$^{-1}$ and 625 mg s$^{-1}$.

| | 312 mg s$^{-1}$ | | | | 625 mg s$^{-1}$ | | | |
|---|---|---|---|---|---|---|---|---|
| $\Delta T$ | 1 K | 0.2 K | 1 K | 0.2 K | 1 K | 0.2 K | 1 K | 0.2 K |
| $u(\Delta\delta m_c)$ | Yes | Yes | No | No | Yes | Yes | No | No |
| $c_1u(y_1)$ | 0.00 | 0.00 | 0.00 | 0.00 | 0.00 | 0.00 | 0.00 | 0.00 |
| $c_2u(y_2)$ | 0.23 | 0.23 | 0.23 | 0.23 | 0.47 | 0.48 | 0.48 | 0.48 |
| $c_3u(y_3)$ | 0.00 | 0.00 | 0.00 | 0.00 | 0.00 | 0.00 | 0.00 | 0.00 |
| $c_4u(y_4)$ | 0.00 | 0.00 | 0.00 | 0.00 | 0.00 | 0.00 | 0.00 | 0.00 |
| $c_5u(y_5)$ | 0.02 | 0.02 | 0.02 | 0.02 | 0.01 | 0.01 | 0.01 | 0.01 |
| $c_6u(y_6)$ | 0.00 | 0.00 | 0.00 | 0.00 | 0.00 | 0.00 | 0.00 | 0.00 |
| $c_7u(y_7)$ | 0.88 | 0.88 | 0.88 | 0.88 | 0.77 | 0.78 | 0.78 | 0.78 |
| $c_8u(y_8)$ | 98.37 | 98.86 | 98.87 | 98.87 | 97.98 | 98.73 | 98.74 | 98.73 |
| $c_9u(y_9)$ | 0.50 | 0.00 | 0.00 | 0.00 | 0.77 | 0.00 | 0.00 | 0.00 |
| $c_{10}u(y_{10})$ | 0.00 | 0.00 | 0.00 | 0.00 | 0.00 | 0.00 | 0.00 | 0.00 |

**Table 6.** Input variables with their distributions used in Monte Carlo simulation.

| $\xi_i$ | $g_i(\xi_i)$ | Annotation |
|---|---|---|
| $I$ | Gaussian | Indication of the balance |
| $T$ | Gaussian | Air temperature in the boundary layer |
| $t$ | Gaussian | Time measurement |
| $p$ | Rectangular | Air pressure |
| $h$ | Rectangular | Air humidity |
| $\delta m_T$ | Rectangular | Effect of the connecting tube |
| $\delta m_L$ | Rectangular | Leakage out of the system |

effect of varying shear stress was obtained with the help of equations (8)–(13) and the mass flow was calculated from equation (6). $\Delta I$ was determined as the slope of the linear fit of the buoyancy corrected balance readings.

Table 7 shows the obtained results as compared with those obtained earlier using the LPU method. The values of the output quantity $y$ (mass flow) and the 95% coverage intervals (CIs) are presented in the table. The distribution of the probability density function of the output quantity is shown in figure 3.

**Table 7.** Comparison of the uncertainty calculation methods at gas mass flow 0.1 mg s$^{-1}$ for MIKES DWS.

| Method | $y$ | $u(y)$ | 95% CI |
|---|---|---|---|
| LPU | 0.0969 | 0.0005 | (0.0959, 0.0979) |
| MCS | 0.0970 | 0.0005 | (0.0961, 0.0979) |

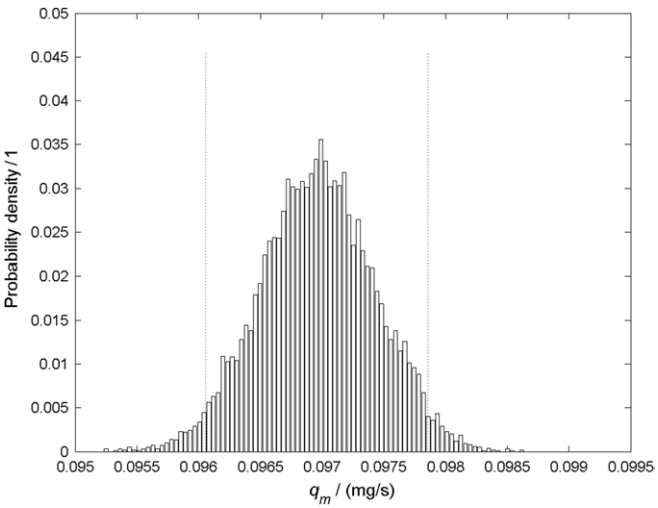


**Figure 3.** The distribution of the probability density function of $M = 10^4$ values of $Y$ at the gas mass flow of 0.1 mg s$^{-1}$.

## 5. Discussion and conclusions

The presented results show that the uncertainty due to the effect of varying shear stress rate at the wall of the gas cylinder is one of the three largest uncertainty components in the dynamic gravimetric gas mass flow measurement at MIKES. The others are the uncertainty due to the parasitic force caused by the connecting tube and the uncertainty of time measurement. These three uncertainty components contribute over 98% of combined standard uncertainty at studied mass flow rates. If $\Delta T$ is small and the flow rate high, then the shear stress related component can be omitted.

The relative contribution of varying shear stress rate increases when the gas mass flow rate decreases. When using the presented uncertainty calculation method and $\Delta T = 1$ K, the contribution is over 92% of the combined standard uncertainty at the gas mass flow of 0.1 mg s$^{-1}$. For the mass flow of 21 mg s$^{-1}$, the contribution decreases to less than 4%. At mass flow rates 312 mg s$^{-1}$ and 625 mg s$^{-1}$ the corresponding contributions are less than 1% at both mass flows. The effect of shear stress increases rapidly when the gas mass flow rate is smaller than 21 mg s$^{-1}$. At the mass flow rates from 312 mg s$^{-1}$ to 625 mg s$^{-1}$ the contribution of the effect is not significant. As can be seen, the contribution of varying shear stress should be taken into account in the uncertainty calculation if the gas mass flow is smaller than 21 mg s$^{-1}$ and temperature variations in the laboratory air may be expected. This is an interesting point, because at higher flow rates the gas (and gas cylinder) cooling is very efficient and it was expected that in this case the effect of shear stress should be taken into account. Due to cooling, the surface temperature is usually monitored for avoiding the dew-point temperature and water condensation on the cylinder wall.

When using the presented theory in estimating the uncertainty due to varying shear stress, the temperature of a

gas cylinder surface is assumed to be known as a function of the measurement time. It is also assumed that the wall of the gas cylinder is isothermal, so the temperature variations at the different locations on the cylinder surface are so small that they can be neglected. This assumption is based on the experiments presented in [6], where the surface temperature of the gas cylinder was studied with the help of a thermographic camera during a measurement cycle. For the temperature measurement, small thermistors with a very short time constant were used with thin connecting wires.

At the small gas flow rates, where the measurement times are long, the pressure decrease in the gas cylinder is not the only probable reason for the temperature difference. It may exist due to unsatisfactory climate control in the wind shield of the system. Also, heat trapped during gas filling may cause the temperature difference, or the temperature in the laboratory may fluctuate due to some other heat source.

To decrease the effect of the varying shear stress rate, the height of vertical surfaces should be minimized. On these surfaces, the velocity fields due to natural convection and shear stress may grow due to temperature differences. Cylindrical objects are traditionally weighed such that the bottom of a cylinder is on the weighing pan of a balance. To minimize the height of the vertical surface, it should be placed by setting the longest side on the weighing pan. Also the isolation of a cylinder with some heat resistive material would reduce the effect, but this is seldom technically feasible.

By looking at the uncertainty estimates for $u(\Delta\delta m_C)$ obtained by time averaging equation (1) and the method based on equations (8) and (9), some observations arise. Assuming that both methods are applied to the first temperature difference model, where $\Delta T = 1$ K, it can be seen that the time averaging of equation (1) gives a similar estimate for $u(\Delta\delta m_C)$ to the method based on equations (8) and (9). However, equation (1) is valid only for vertically placed cylinders and it cannot be applied to any other cylinder positions.

The presented calculation method for the varying shear stress is used for obtaining an uncertainty estimation. This method includes many assumptions (for example, isothermal cylinder walls) and simplifications (for example, two-dimensional solution for a flat plate or stagnation point flow) which are taken into account in calculating the combined standard uncertainty of the method. In [6], a value of $u_c(\tau_w(\Delta T)) = 0.7\,\text{mPa K}^{-1}$ is obtained at $\Delta T = 1$ K.

As can be seen from table 7, the LPU and MCS give practically the same values for output quantity, uncertainty estimate for the output and 95% CI. The possible effect of correlated input variables seems to be negligible.

Based on the results and analysis presented in this study, the effect of varying shear stress should be taken into account in the uncertainty calculation. If the temperature difference between the gas cylinder and ambient air increases or decreases during the gas mass flow measurement, a careful inspection of the measurement result and the corresponding uncertainty is even more vital.

## References


[1] Gläser M and Do J Y 1993 *Metrologia* **30** 67–73
[2] Gläser M 1990 *Metrologia* **27** 95–100
[3] Löfström P-H 1999 Characterisation of a system that measures gas samples using a mass flow meter *SP Report* 1999:12 Borås, Swedish National Testing and Research Institute pp 57
[4] Mana G, Palmisano C, Perosino A, Pettorruso S, Peuro A and Zosi G 2002 *Meas. Sci. Technol.* **13** 13–20
[5] Sillanpää S, Niederhauser B and Heinonen M 2006 *Measurement* **39** 26–33
[6] Sillanpää S and Heinonen M 2007 *Exp. Thermal Fluid Sci.* **32** 459–66
[7] BIPM, IEC, IFCC, ISO, IUPAC, IUPAP and OIML 1993 *Guide to the Expression of Uncertainty in Measurement* (Geneva: International Organisation for Standardisation) p 101
[8] Schlichting H and Gersten K 2000 *Boundary Layer Theory* 8th edn (Berlin: Springer) pp 265–75
[9] Pop I and Takhar H S 1993 *Z. Angew. Math. Mech.* **73** 534–9
[10] BIPM, IEC, IFCC, ISO, IUPAC, IUPAP and OIML 2004 *Guide to the Expression of Uncertainty in Measurement—Supplement 1: Numerical Methods for the Propagation of Distributions* (Geneva: International Organisation for Standardisation) p 42
[11] Davis R S 1992 *Metrologia* **29** 67–70